ASE-1637

RESULTS OF A SOUNDING ROCKET EXPERIMENT TO STUDY CELESTIAL X-RAY SOURCES

H. GURSKY

R. GIACCONI

P. GORENSTEIN

J. R. WATERS

CONTRACT NO. NASw-1535

PREPARED FOR

NATIONAL AERONAUTICS AND SPACE ADMINISTRATION

AMERICAN SCIENCE AND ENGINEERING

11 Carleton Street, Cambridge, Massachusetts 02142

AS&E

ASE-1637

RESULTS OF A SOUNDING ROCKET EXPERIMENT TO STUDY CELESTIAL X-RAY SOURCES

By H. Gursky, R. Giacconi, P. Gorenstein and J. R. Waters

Prepared under Contract No. NASw-1535 by
AMERICAN SCIENCE AND ENGINEERING
11 Carleton Street, Cambridge, Massachusetts 02142

for
NATIONAL AERONAUTICS AND SPACE ADMINISTRATION

FOREWORD

This document is the final report on Contract No. NAS w-1535, which called for the reduction and analysis of data obtained from NASA Aerobee 4.148, which was flown from the White Sands Missile Range on 8 March 1966. The rocket payload was developed at AS&E under NASA contract NAS w-1284. The objective of the program was to study celestial x-ray sources with instrumentation of high intrinsic angular resolution and the particular x-ray source studied was the Crab Nebula.

ACKNOWLEDGEMENTS

Part of this work represented a joint effort with scientists at the Massachusetts Institute of Technology. The participation scientists were, Professor H. Bradt, Professor G. Garmire, Professor M. Oda, Dr. B.V. Sreekantan, and Dr. G. Spada. Results of this joint effort have been reported in the April 1967 issue of the Astrophysical Journal.

We wish to acknowledge the support in this work of Mr. G. Ouellette, who was responsible for many of the astronomical calculations presented here, Mr. M, Bate, who was responsible for the computer programming effort, and Mrs. J. Zmijewski and Miss T. Arczynski, who did most of the data scanning and the computational work.

We wish to acknowledge many fruitful discussions with Dr. M. Annis, Dr. J. Carpenter, Dr. S. Frankenthal, and Dr. O. Manley of AS&E; Professor Bruno Rossi, Professor B. Burke, and Professor P. Morrison of M.I.T. , and Professor L. Woltjer of Columbia University.

INTRODUCTION

The results presented here are the continuation of an observational program of x-ray astronomy that began at AS&E in 1961. Observations have been entirely with Sounding Rockets, but two satellite experiments are in various stages of completion for future work. The present experiment was performed from an Aerobee rocket flown from the White Sands Missile Range on 8 March 1966. The payload was developed under contract NAS w-1284 and has been described in the final report on that contract in ASE Document 1372 (September, 1966).

The objective of this experiment was the study of an individual x-ray source with instruments capable of very high angular resolution. Although x-ray optics are feasible and are presently being used in solar studies, limitations of pointing accuracy and observation time prevented their use on sounding rockets for experiments on even the strongest celestial x-ray sources. Instead, the experiment utilized modulation collimators in which high resolution is achieved by shadowing of a series of wire grids. This device was originally devised by Professor M. Oda of M.I.T. and was developed at M.I.T. and AS&E. The device was first used on AS&E rocket experiments of 28 August 1964 and 24 October 1964 and resulted in the measurement of the angular size of Sco X-1. The collimator used in the present experiment had an angular resolution of 40 arc seconds, compared to about 30 arc minutes of those used earlier. In addition to high resolution in x-rays, the payload was equipped to measure vehicle attitude very precisely by photographing stars.

The x-ray source chosen for this study was the Crab Nebula. Excluding the solar system, the Crab Nebula is perhaps the most widely studied object in the sky. It is apparently the expanding remnant of a supernova explosion that was probably recorded by far-eastern observers in 1054 A. D. It is presently very bright optically and in radio. Its importance in astronomy is that it was the first object that provided clear-cut evidence that the synchrotron process (radiation by relativistic electrons in a magnetic field) was a very significant means of energy dissipation in celestial objects. This observation, in turn, implies that the Crab is filled with very high energy electrons and a relatively strong magnetic field. Observations of the Crab, have in turn, led to speculation of the role supernova explosionsplay

on more gross features of the galaxy. Shklovskii[1] speculates that high energy particles escaping from the immediate vicinity of supernova remnants are the primary source of galactic cosmic rays, and Oort[2] has suggested that high-velocity clouds of hydrogen observed in radio are the very ancient ejecta of, or the interstellar matter swept out by a supernova explosion.

In spite of the wealth of observational data on the Crab, no well defined model of the object obtains; in particular, the means by which the original kinetic energy of the supernova explosion is converted into electrons and magnetic field is not known. The following is a summary of the observational data on the Crab:

1) In visible light, the Crab has a dual character. The continuum radiation (which is the synchrotron radiation) comprises an almost featureless region of several arc minutes extent. The spectral line radiation comes from a series of filaments that appear to encompass the region.

2) The continuum radiation is highly polarized, in certain regions by as much as 20% and even averaged over the entire nebula, the degree of polarization is 7%.

3) Dynamical effects are seen in the Crab. The object is observed to be expanding at a rate of $\sim 10^3$ km/sec. Light "ripples" (regions of enhanced surface brightness) are seen to traverse the central region of the nebula in times of the order of several months.

4) In radio, the Crab appears to be about the same size as in visible. Observations in radio are greatly hampered by the poor angular resolution of existing radio telescopes. Early measurements based on observations during lunar occultations of the Crab indicated its radio size to be significantly larger than its size as seen at optical frequencies. More recent observations fail to detect any significant difference in size, although there is still only poor data available on the shape of the Crab in radio.

5) The radio emission from the Crab is observed to be polarized. At high frequency, the degree of polarization is found to be essentially the same as it is in visible light, although the center of polarization appears to be displaced from the optical center of the Crab by about 1 arc minute. The polarization decreases with decreasing frequency apparently as a result of differential Faraday rotation in the Nebula.

6) A small diameter (< 20") radio source is observed within the Crab at very low frequencies. Hewish and his co-workers at Cambridge have recently located this component close to the optical center of the Crab with a precision of about 1 arc minute. The radiation in this small diameter region cannot be explained by the synchrotron process, and its origin is not understood.

7) The continuum radiation is known to extend into the infrared on the basis of direct observations, and is inferred to extend well into the extreme ultraviolet (several hundred angstroms) on the basis of observations of certain spectral lines that can only be excited at high energies.

In x-rays, evidence for a source at the Crab was first presented by Gursky, Giacconi, Paolini, and Rossi[3], based on a rocket observation of October 1962, and by Bowyer, Byram, Chubb, and Friedman[4], based on observations during April 1963. The Crab was positively identified as an x-ray source by Bowyer et al.[5], who observed its occultation by the moon. Based on the data from this latter experiment, Bowyer et al. stated that the center of the x-ray source lay on a line (coinciding with the limb of the moon at the time that the source was being traversed) that passed within 30" arc of the optical center and that the x-ray emission region was of one arc minute extent. The precision of these results was not stated. These results were modified by Finn, Manley, and Ouellette[6], based on a re-analysis of the lunar position and apparent motion. These authors took into account the motion of the rocket (the position of moon varies by about 1" arc for each mile on the surface of the Earth) and showed that the lunar limb was displaced about 1' arc from where it had originally been placed (it still was 30" arc from the optical center of the Crab) and that since the apparent rate of motion of the limb was almost twice that originally calculated, the angular extent of the x-ray source was two minutes of arc. This re-analysis simply corrected a systematic error in the astronomical quantities used in the analysis and did not affect the basic precision of the results.

Other x-ray observations of the Crab showed that its spectrum extended to very high energies (~ 100 keV)[7][8], with an apparent power law dependence, and demonstrated that at the present time, the Crab is expending as much power in x-rays as it is in visible light.

The attempt in the present experiment was simply to measure the size and position of the x-ray source in the Crab with as high an angular resolution and precision as could be attained with existing techniques, and to obtain two dimensional data on these quantities as opposed to one dimensional data as was obtained in the occultation experiment.

The relevance of these measurements is simply that these two parameters, angular size and position, are two of the most important properties of the x-ray source needed in beginning to construct a theory for the x-ray emission from the object,

It is natural to assume that the x-rays in the Crab are originating as synchrotron radiation, the dominant process at lower frequencies, [9][10] Electrons of energy $\sim 10^{11}$ ev in a magnetic field of $\sim 3 \times 10^{-4}$ gauss are required to give the observed optical and radio continuum. In order to generate x-rays, either the electron energy must be increased to $\sim 10^{13}$ ev in the same magnetic field, or the intensity of the magnetic field must be increased by about a factor of ten in certain regions. In either case, the lifetime of the electrons (ratio of kinetic energy to rate of energy loss) becomes only the order of a year. This implies a remarkably efficient means of accelerating the electrons to such high energies, or that the electrons spend only a small time in regions where the x-rays are produced.

It is also possible to construct x-ray models for the Crab based on thermal bremsstrahlung as the production mechanism[11][12]. In this case, the Crab would be pervaded by a plasma of temperature $> 10^{8}$°K, which is presumably the remnant mass of the object that originally exploded. The mass of the plasma is strongly dependent on the average atomic weight and could be in the vicinity of $1 M_{\odot}$.

The critical points of comparison between these models are as follows:

1. Line Emission - Thermal bremsstrahlung invariably produces some line emission in the x-ray spectrum, whereas synchrotron radiation yields a featureless spectrum. The shape of the continuum is not a good indicator for distinguishing between the two processes; the shape simply limits the electron spectrum, distribution of temperature, etc., or whatever parameters go into the spectral distribution function.

2. Polarization - Synchrotron x-rays would be expected to be polarized, bremsstrahlung x-rays would not.

3. Depolarization - A hot plasma would depolarize radio continuum produced within the plasma region by differential Faraday rotation. In principal, by observing the depolarization, the regions containing plasma can be traced out.

4. Time Variability - Generally very large differences in life-times are derived for hot plasmas (~ 1000 years) compared to relativistic electrons (~ 1 year). Observations of time variability on a short time scale, would favor the synchrotron process.

The results of the present experiment are given in Appendix A, which is the text of an article published in the Astrophysical Journal (148, L5, 1967). The article also gives a description of the experiment and the methods of analyzing the data. There were two principal results:

1) The x-ray emission region was found to be of finite size. The most probable size was 2' x 1' of arc, with the larger dimension coinciding with the larger dimension of the optical Crab, but the results were not inconsistent with a distribution in x-rays identical to the distribution in visible light.

2) The centroid of the x-ray emission region was located with a precision of about 15" arc and was found to coincide with the centroid of the distribution in visible light.

The significance of these results is that the very similar appearance in x-ray and optical frequencies implies an intimate connection in terms of the physical processes giving rise to the two. It does not mean necessarily that the same physical process is giving rise to the observed radiation, but rather, for example, that the same physical process is responsible for accelerating the electrons that gives rise to the optical synchrotron radiation as is (or was) heating the plasma that yields the x-ray bremsstrahlung. Furthermore, it should be possible now to calculate with some certainty what kind of depolarization in the radio should be seen based on a thermal bremsstrahlung model for the x-rays.

Additional work done on this contract was the spectral distribution of the x-rays from Sco X-1 in the energy range 2-10 keV as obtained from the analysis of proportional counter data obtained during two rocket flights (NASA Aerobee 4.148 and 4.149). The results are contained in Appendix B. The data were fitted to three kinds of spectra and the best was obtained in both cases to an exponential spectrum characteristic of the thermal bremsstrahlung process, although other processes cannot be excluded. The temperature in the exponent was found to be about 3.5 x 10^7°K in the case of the data from flight 4.149 in

which Argon filled counters were used, and 6.4×10^{7} K in the other flight when Xenon counters were used. The difference may reflect systematic errors that are not accounted for in the data or may indicate that the spectrum cannot be described by a single temperature. The Xenon data covers a much broader energy range than does the Argon data.

REFERENCES

1. Shklovskii, I. S., Cosmic Radio Waves (Harvard Univ. Press, Cambridge, Massachusetts 1960) p. 328 ff

2. Oort, J. H., Interstellar Matter in Galaxies (W.A. Benjamin, New York, 1962, L. Woltjer, Ed.) p. 3 ff

3. Gursky, H., Giacconi, R., Paolini, F.R., and Rossi, B. Phys. Rev. Letters 11, 530, (1963)

4. Bowyer, S., Byram, E.T., Chubb, T.A., and Friedman, H. Nature 201, 1307, (1964).

5. Bowyer, S., Byram, E.T., Chubb, T.A., and Friedman, H. Science 146, 912, (1965).

6. Finn, R., Manley, O.P., Ouellette, G., Appendix H in ASE-2017 (American Science and Engineering, Cambridge, Massachusetts 1966).

7. Clark, G., Phys. Rev. Letters 14, 91, (1965).

8. Peterson, L.E., Jacobson, A.S., Pelling, R.M. Phys. Rev. Letters 16, 142, (1966).

9. Shklovskii, I.S., Sov. Ast. 10, (1966).

10. Woltjer, L., Ap. J. 140, 1309, (1964).

11. Morrison, P., and Sartori, L., Phys. Rev, Letters 14, 771, (1965).

12. Morrison, P., and Sartori, L., "Thermal X-rays from Non-Thermal Radio Sources", Preprint, April 1967, Submitted to Ap. J.

APPENDIX A

Submitted for publication on February 10, 1967 to the Editor of the Astrophysical Journal

MIT/ASE-1542

THE SIZE AND POSITION OF THE X-RAY SOURCE IN THE CRAB NEBULA

M. Oda*, H. Bradt, G. Garmire**, G. Spada†, B.V. Sreekantan††
Massachusetts Institute of Technology
Cambridge, Massachusetts

and

H. Gursky, R. Giacconi, P. Gorenstein, and J.R. Waters
American Science and Engineering
Cambridge, Massachusetts

*Presently at Institute of Space and Aeronautical Science, University of Tokyo, Tokyo, Japan

**Presently on leave at California Institute of Technology, Pasadena, California

†On leave from the Laboratorio di Astrofisica, Frascati, Italy

††Presently at the Tata Institute of Fundamental Research, Bombay, India

During a recent rocket flight, we observed the 1 to 6 keV x-radiation from the Crab Nebula with a modulation collimator of high resolution. We find the emission region to be centered on the Crab and of finite size. These results are in agreement with those of the lunar occultation experiment carried out by Bowyer, Byram, Chubb, and Friedman (1964). The present measurement improves upon the earlier work in that it provides size and position information along two nearly perpendicular directions rather than the one direction of the lunar transit. Also, since the measurements of Sco X-1 (Gursky, Giacconi, Gorenstein, Waters, Oda, Bradt, Garmire, and Sreekantan 1966a, 1966b) and the Crab Nebula were made with the same instrument during a single flight, we were able to directly observe the qualitatively different appearance in x-rays of a star-like source (Sco X-1) and a source of finite angular size (Crab).

The Crab Nebula was first positively identified as a strong X-ray source by the above mentioned occultation experiment. Thus the Crab is now known to be bright in a frequency range from 10^7 to 10^{19} c/s. In the radio and optical regions, the radiation is believed to be synchrotron emission because of the observed high degrees of polarization. Although it has been argued that the observed x-rays represent an extension of the synchrotron radiation to higher energies (Woltjer 1964; Shklovskii 1966), there is no conclusive evidence that eliminates other possibilities, notably thermal emission from a hot plasma. Arguments in support of this latter mechanism have recently been presented by Morrison and Sartori (1967). In any case, the gross dynamics of the Crab Nebula must be affected in a significant way by the x-ray emission since the total radiated power in x-rays is comparable to that at optical wavelengths and greatly exceeds that at radio wavelengths. Thus, comparison of the detailed angular structure in the x-ray, optical, and radio regions should contribute materially toward our understanding of the Crab Nebula.

The data reported here were obtained during a sounding rocket flight on 8 March 1966. Observations of the bright x-ray source in Scorpio, Sco X-1, during the same flight yielded both a 20" upper limit to its angular size and its position to a precision of four square arc minutes (Gursky, et. al. 1966a, 1966b) which, in turn, made possible an identification of its optical counterpart (Sandage, Osmer, Giacconi, Gorenstein, Gursky, Waters, Bradt, Garmire, Sreekantan, Oda, Osawa, and Jugaku, 1966). Both the Crab and Scorpio observations were made with the same optical - x-ray sensor system. It consisted of proportional counters with 50μ Be windows and 30 mg/cm^2 of Xenon, a camera, and two four-grid modulation collimators, each with multiple 40" x 10° (FWHM) angular transmission zones, or "bands", separated one from another by about 5'. These angular dimensions differed for the two (one "long" and one "short")

collimators by about 5 percent to provide a vernier effect which in principle permits one to identify the angular transmission band corresponding to a given peak in the x-ray data. The 16mm camera took successive one second exposures and simultaneously viewed a $12^{o} \times 8.5^{o}$ star field and a portion of each collimator. The collimators were illuminated by a diffuse light source in such a way that the x-ray transmission bands were imaged directly onto the image of the star field. This allowed us to project lines of position corresponding to each data peak directly onto the celestial sphere. The entire detection system viewed the sky through the front end of the Aerobee 150 rocket.

The observations were made in the following way. The rocket was pointed toward the Crab Nebula for a period of about 40 seconds during which the jitter in the attitude control system caused the rocket to scan the Nebula at rates of several arc minutes per second. Directly following this sequence, the rocket was rolled 60^{o} about its long axis, and a 40 sec "postroll" period provided data which yielded lines of position on the celestial sphere which cross at 60^{o} those obtained during the "preroll" period. During the preroll and postroll periods there were, respectively, nine and four transits of the optical Crab by the transmission bands of the short collimator. The long collimator made, respectively, nine and five transits during these periods.

The individual transits of the source did not appear as statistically significant peaks in the counting rate data. Therefore, the optical aspect data, precise to 15", was used to sum the data from the successive transits of the source region. For both the short and long collimators, the angular interval between two successive transmission bands was divided into 20 equal bins, each of approximately 15" width. Both systems of 20 bins were fixed upon the celestial sphere, essentially superimposed, with bin #10 centered at (1950.0) $\alpha = 5^{h}\ 31^{m}\ 30^{s}$, $\delta = 21^{o}\ 59'$, the coordinates listed in the Becvar Catalog for the center of the Crab Nebula. In order to reduce the effects of background counts, we restricted the energy region studied to 1 to 6 keV. Each detected x-ray was credited to the bin which at that moment was being traversed by the center of a collimator transmission band. Also, the total time spent in each bin was accumulated. This superposition was carried out separately for each of the two collimators ("short" and "long") for both the preroll and postroll periods. The resultant rates with statistical errors are presented in Figure 1.

The centroid of the peak in each of the four sets of data in Figure 1 lies close to bin #10. Thus, in both scan directions, the center of the x-ray source lies close to the center of the Crab. We further note that the occurrence of the "long" and "short" peaks at the same bin number eliminates

from consideration most of the other celestial positions which, due to the multiplicity of transmission directions through the collimator, might be candidates for the location of the x-ray source. The background rates indicated in Figure 1 with their statistical errors were calculated from the rates in the 8 or 9 bins most removed from the peak. In each case they are consistent with the rates of about equivalent statistical significance obtained during the gross maneuvers of the rocket prior to and subsequent to the Crab observations.

In order to obtain celestial positions and angular sizes based on the entire data we superimposed the short and long data bin by bin for both the preroll and postroll observations (Figure 2). Since the angular sizes of the long and short bins are different by 5 percent, the straightforward bin by bin superposition smears the angular resolution, but at most by 7" (1/2 bin) in bin #1 and bin #20. The effect on the rates is negligible. In Figure 2 we also show the expected responses with normalized areas of point sources and of rectangular sources of uniform intensity which best fit the data. In the case of the preroll data the most probable angular size is 60" $\pm$ 60" for the assumed rectangular shape. However, we cannot exclude a point source. During the postroll period the source spent a greater fraction of the time within the 40" transmission zones. The data is therefore of better quality and yields an angular size of 110 $\pm$ 25". In this case a point source is clearly excluded. The quoted errors are based upon χ^2 tests of other source sizes and represent a probability of occurrence equal to that expected for one standard deviation in a normal distribution. As we will discuss later, these data are also consistent with an x-ray source region identical in shape and size to that of the optical source.

The total counting rates due to the source in the 1 to 6 keV region are 1.1 ± 0.3 cm^{-2} sec^{-1} and 2.1 ± 0.3 cm^{-2} sec^{-1} for the preroll and postroll data respectively. These rates include the effects of the limited angular aperture (40" FWHM) of the collimators and the reduction of effective counter area by the x-ray shadows of the collimator, grid, and counter window support structures. The stated precision in these rates is statistical and arises, in part, from the statistical errors in the background measurements. The apparent discrepancy in the rates can be understood either as a statistical fluctuation in their difference of two standard deviations or as systematic errors in our initial assumptions as to which bins in Figure 1 represent true measurements of the background. We have found, however, that our conclusions regarding the size and location of the source are not significantly affected by the assumption of any other set of background levels which are compatible with the flight data.

To test this method of analysis we have carried out the same superposition techniques on the Sco X-1 data obtained later in the same flight (Figure 3). The data indeed conform to a point source with a precision of about 15", and as previously reported, the line of position corresponding to the centroid of the peak lies within 20" of the optical object Sco X-1.

The celestial position of the center of the Crab x-ray source is obtained from the intersection of the lines of position corresponding to the centroids of the peaks in Figure 2:

$$\alpha \quad (1950.0) = 5^h\ 31^m\ 30^s$$

$$\delta \quad (1950.0) = 21^\circ\ 59.1'$$

The statistical errors (standard deviation) in the centroid determinations are 20" and 15" in the preroll and postroll data respectively. The 15" error in each of the many aspect determinations is random and produces negligible error in the centroid position. We previously estimated (Gursky, et. al. 1966b) that a systematic error of as much as 30" could be introduced by uncertainties in the correlation of the optical fiducial pattern with the x-ray transmission directions and, probably more important, by errors in extrapolation across the film. We now believe that systematic errors in the Crab are somewhat smaller because (1) the discrepancy between the position of the optical object Sco X-1 and the position deduced from the flight data was, as mentioned above, only about 20" and (2) the position of the Crab lay closer to the center of the field of view than did Sco X-1.

The position and size results from this experiment are presented schematically in Figure 4. The darkly shaded area represents the most probable x-ray source region. Because of the large statistical error in the preroll size result we choose to report the circular area as an idealization of the size and shape of the x-ray source. Its diameter (100") is obtained from a statistical weighting of the preroll and postroll data.

In Figure 5 we have transferred these results to a Palomar photograph of the Crab Nebula. The earlier results based on the occultation experiment are also shown. The dashed line, marked NRL, gives the originally reported (Bowyer, et. al. 1964) position of the lunar limb corresponding to the observed peak of the x-ray distribution. Manley and Ouellette (1965) have recently recalculated the lunar position taking into account parallax introduced by the rocket motion during the flight and their result is the solid line marked NRL. The effect of this parallax was to cause the limb of the moon to almost double its rate of traversal across the Crab and this, in turn, gives rise to an angular size of about 2' rather than about 1' as originally reported.

In order to make a more quantitative comparison between the distribution of visible light and x-rays we integrated the light intensity in the directions normal to our x-ray scans using a contour map given by Woltjer (1957). The results are shown in Figure 6. It is seen that the centroids of the x-ray and visible light distributions agree well within the random error of the x-ray observations. We find that x-ray distribution functions of the same size and shape as the visible light distributions can easily be fit (with resulting χ^2 probabilities of 60 percent and 30 percent) to the preroll and postroll data.

In summary, this experiment yields **two** principal results. First, the x-ray and visible light distributions have a common center within the 15" precision of the measurement. Second, the source has a finite angular extent. The data are consistent with x-ray emission regions which range in size and shape from uniform emission by the central two arc minutes of the Crab to a distribution identical to that of the visible light. These results place constraints upon the details of the possible models for x-ray emission. For instance, the markedly off-center features of the Crab, such as the maximum of the radio polarization at centimeter wavelengths (Gardner, 1965; Allen and Barrett, 1966) or the small diameter radio source at 25 - 40 mc/s (Hewish and Okoye 1965; Andrew, Branson, and Wills 1964), cannot be made to have a direct simple relation to the x-ray production.

ACKNOWLEDGEMENTS

We wish to thank the staffs of American Science and Engineering and of the Laboratory for Nuclear Science at M.I. T. for their assistance throughout this experiment. We are grateful to Dr. Leo Sartori, Professor Philip Morrison, Professor L. Woltjer, and Dr. Oscar Manley for helpful discussions. We are further grateful for the support given us by the staffs of the Sounding Rocket Branch of Goddard Space Flight Center and the White Sands Missile Range. This work was supported in part through funds provided by the National Aeronautics and Space Administration under contracts NASw-1284 and NASw-1535 and grant NSG-386, and in part by the U. S. Atomic Energy Commission under contract AT(30-1)2098.

REFERENCES

Allen, R. J., and Barrett, A. H. 1966, presented at 123rd meeting of the AAS, Los Angeles (abstract to be published in A. J.).

Andrew, B. H., Branson, N. J. B. A. and Wills, D. 1964, Nature, 203 171.

Bowyer, S., Byram, E. T., Chubb, T. A. and Friedman, H. 1964, Science, 146, 912.

Gardner, F. F. 1965, Australian J. Phys., 18, 385.

Gursky, H., Giacconi, R., Gorenstein, P., Waters, J. R., Oda, M., Bradt, H., Garmire, G. and Sreekantan, B. V. 1966a, Ap. J., 144, 1249.

_____1966b, Ap. J. 146, 310.

Hewish, A. and Okoye, S. E. 1965, Nature, 207, 59.

Manley, O. and Ouellette, G. 1965, private communication.

Morrison, P. and Sartori, L. 1967, to be published.

Sandage, A. R., Osmer, P., Giacconi, R., Gorenstein, P. Gursky, H., Waters, J. R., Bradt, H., Garmire, G., Sreekantan, B. V., Oda, M., Osawa, K. and Jugaku, J. 1966, Ap. J., 146, 316.

Shklovskii, I. S. 1966, Astr. Zh., 43, 10 (English trans. in Soviet Astr. - A. J., 10, 6, 1966).

Woltjer, L. 1957, B. A. N., 13, 302.

Woltjer, L. 1964, Ap. J., 140, 1309.

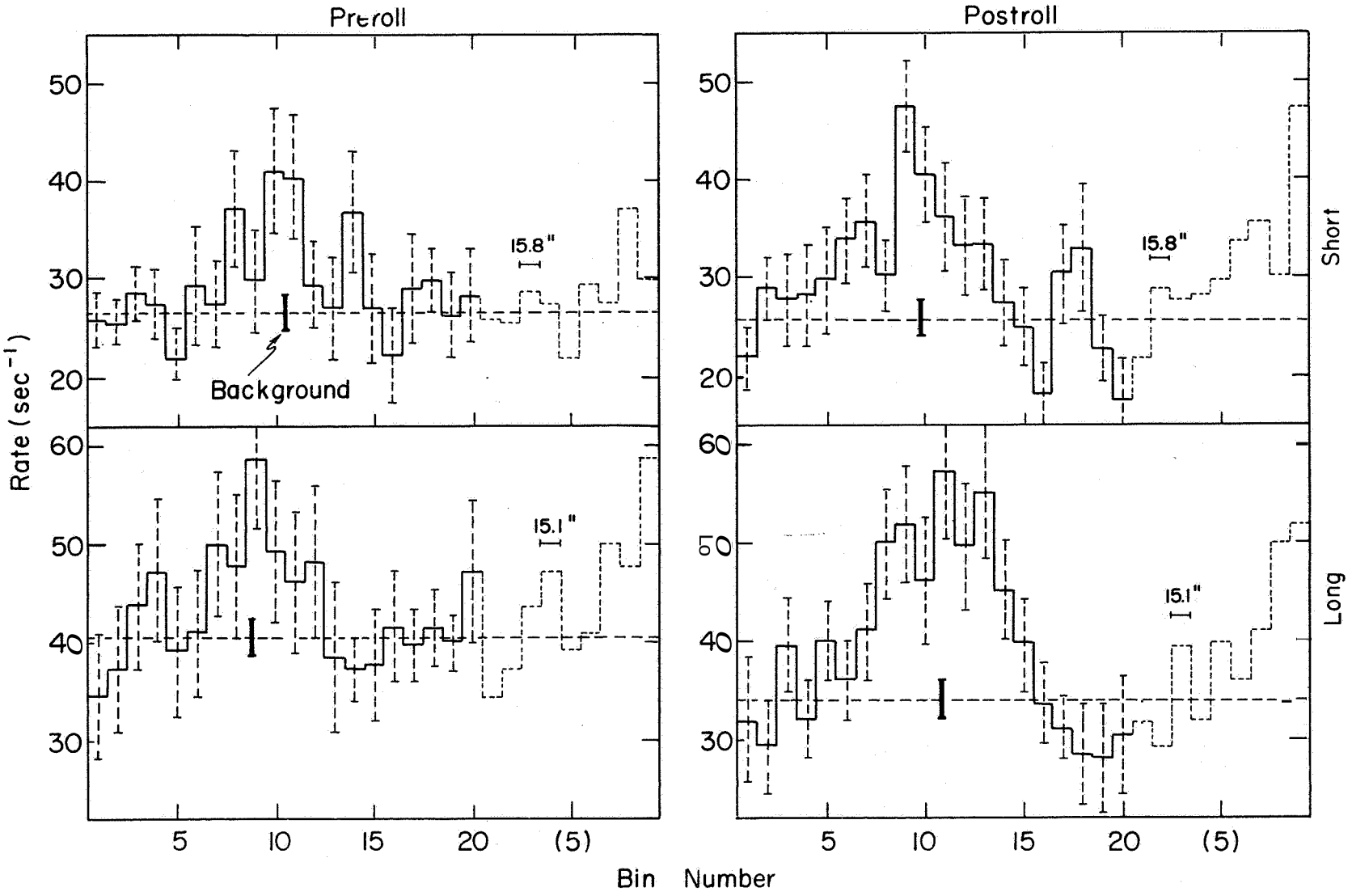

Figure 1: Data after initial superposition with periodicity equal to the angle of separation between adjacent transmission directions, namely 5'1.91" and 5'16.62" for the long and short collimators respectively. These angular intervals are divided into 20 equal bins and, in each histogram, the center of bin #10 represents the Becvar coordinates for the center of the Crab Nebula.

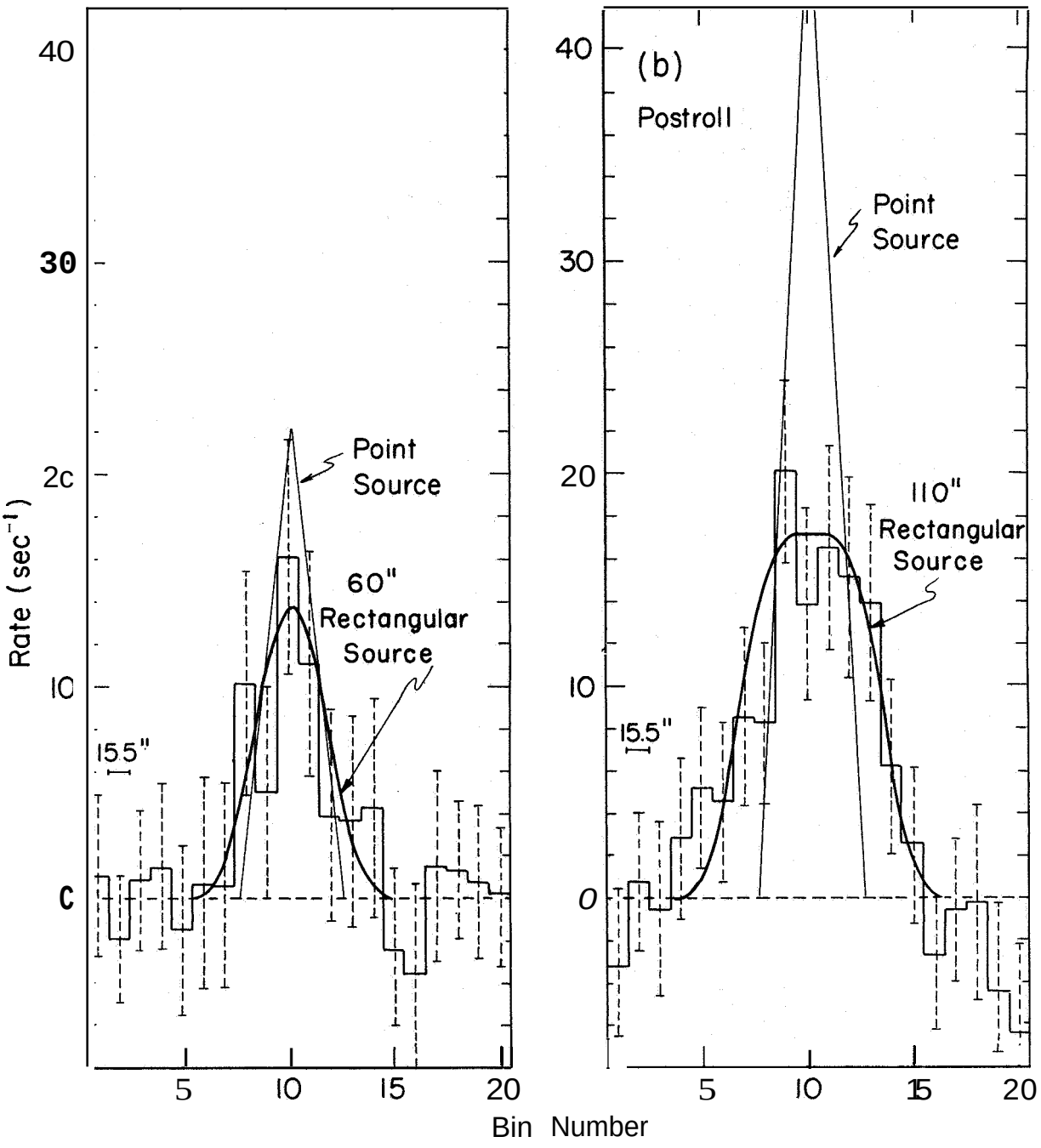

Figure 2: Summation of all data obtained during the preroll (postroll) hold on the Crab Nebula, plotted with background subtracted as a function of bin number. The error bars indicate one standard deviation and include the effect of the uncertainty in the background rates. The bin width (15.46") is the mean of the long and short bin widths. The expected responses for point and rectangular source distributions are also presented.

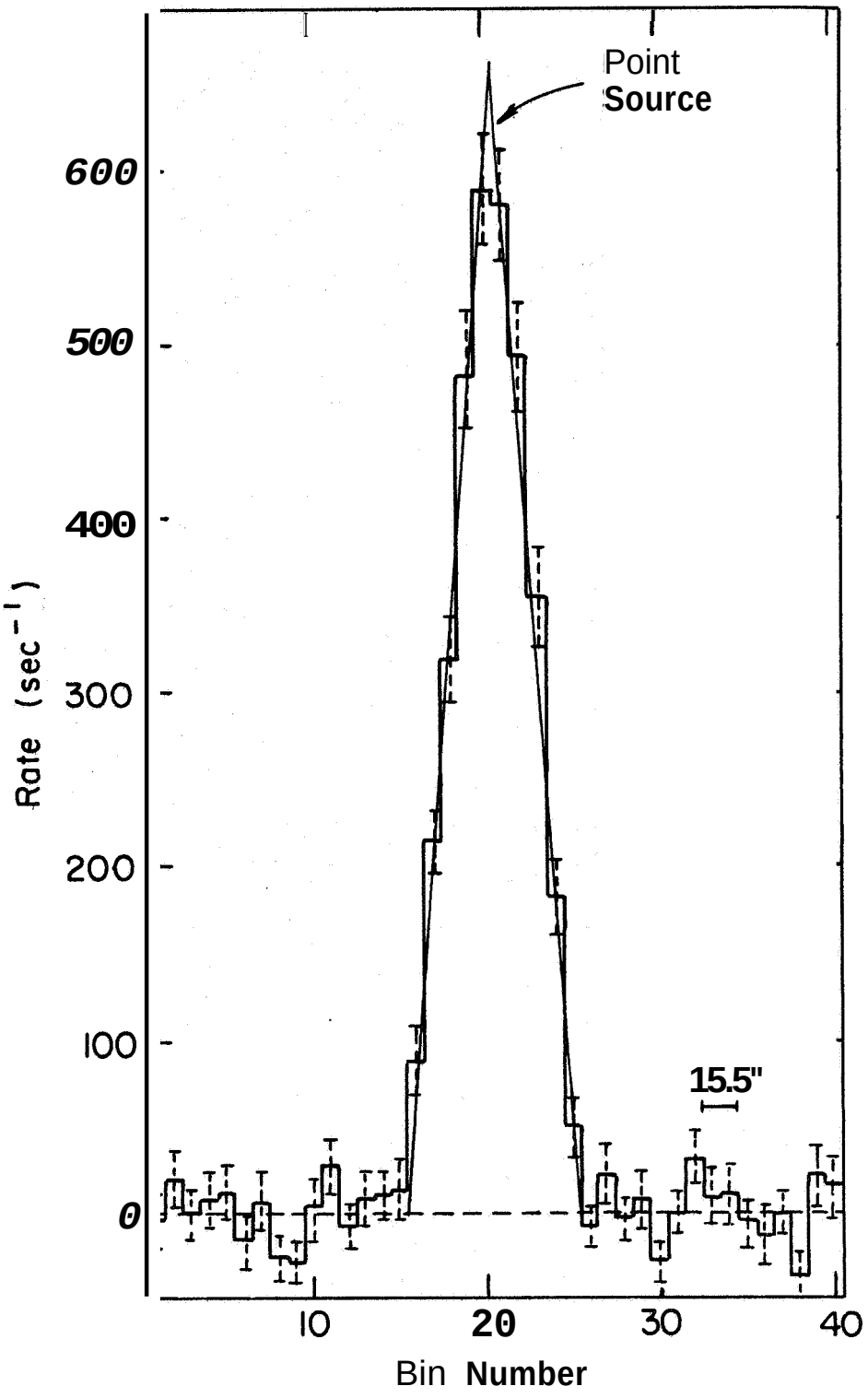

Figure 3: Superposition of all data obtained during "hold" portion (289<t<302 sec) of the *Sco* X-1 observations described by Gursky et.al. (1966a, 1966b).

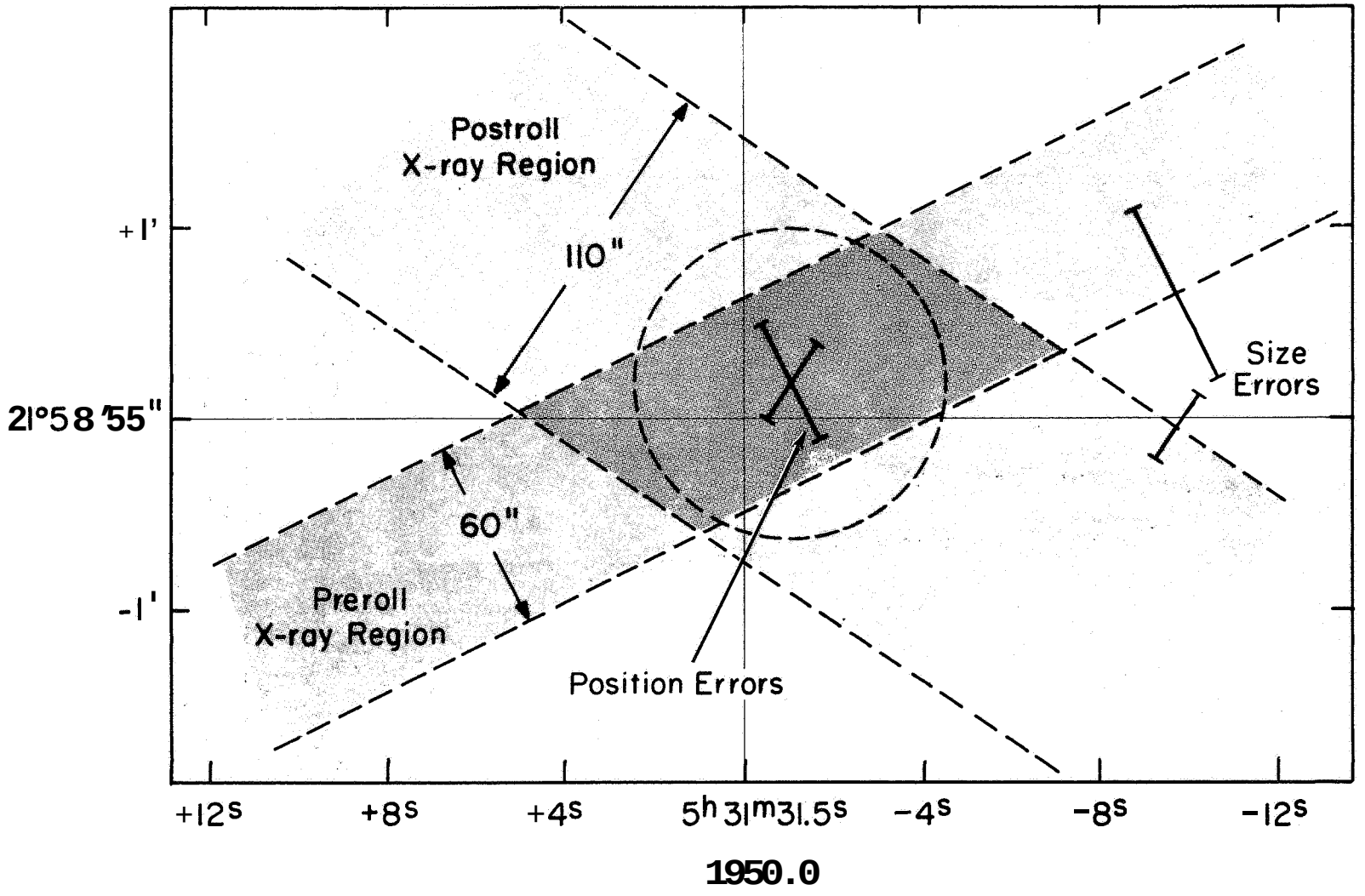

Figure 4: Celestial coordinates of the x-ray results presented in Figure 2. The two lightly shadowed bands indicate the x-ray regions defined by the preroll and postroll scans respectively under the assumption of rectangular source distributions in each scan direction. The darkly shadowed area of intersection indicates the most probable x-ray source region under these assumptions. The error bars represent the statistical errors; the systematic errors in the position are estimated to be less than 15". The size and shape of the source is idealized as a circular area of diameter 100". The origin of the coordinate system is the southwest component of the central double star.

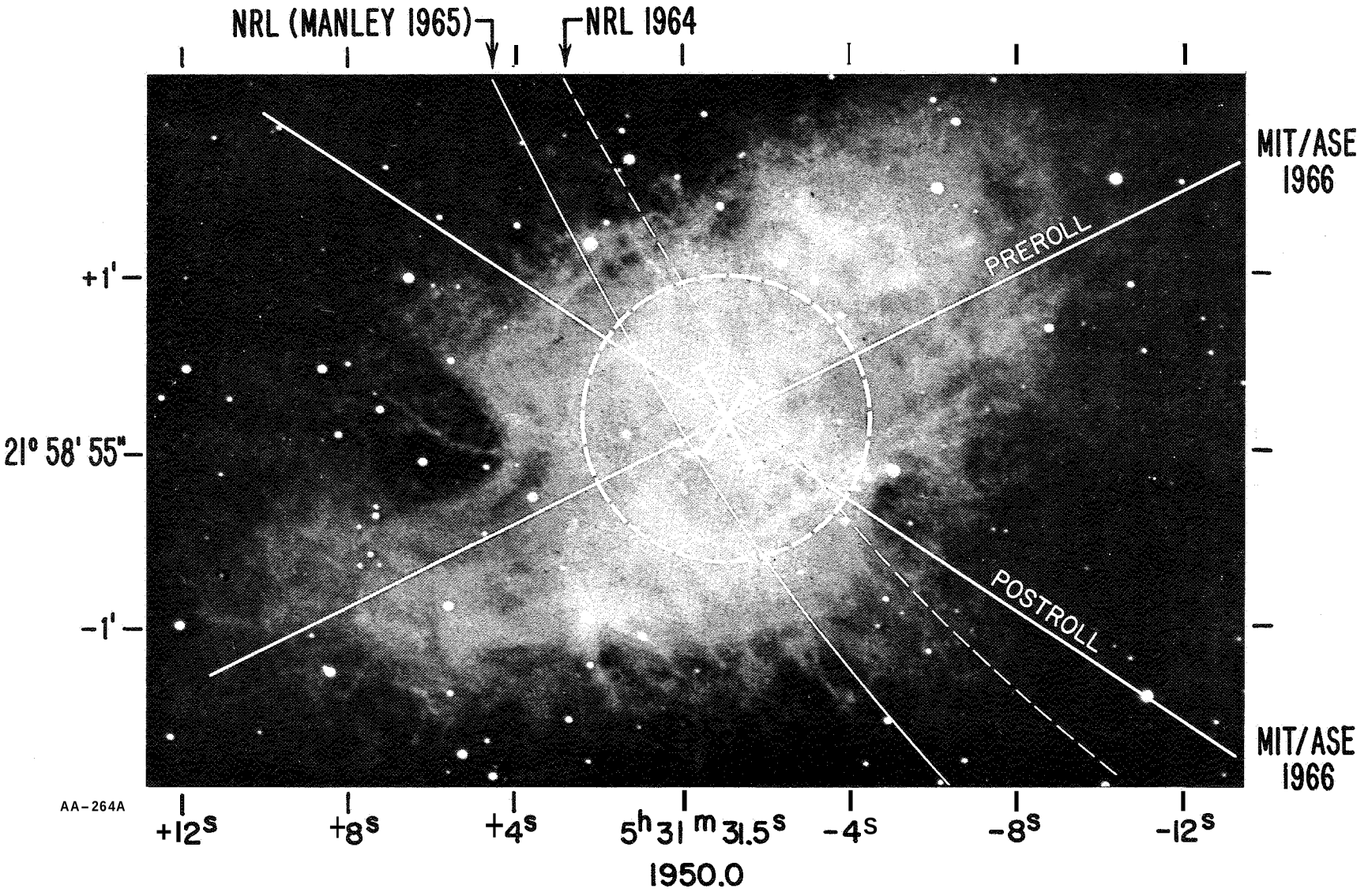

Figure 5: Summary of results pertaining to the position of the x-ray source in the Crab Nebula. The dashed curved line is the line of position obtained from a lunar occultation experiment by Bowyer, ~~et. al.~~ (1964), and the solid curved line is the same result corrected by Manley and Ouellette (1965) for parallax due to the motion of the rocket. The intersection of the two MIT/AS&E lines of position is at (1950.0) $\alpha = 5^h\ 31^m\ 30^s$, $\delta = 21°\ 59.1'$. The 100" diameter circle, taken from Figure 4, is an idealization of the source region. The origin of the coordinate system is the southwest component of the central double star.

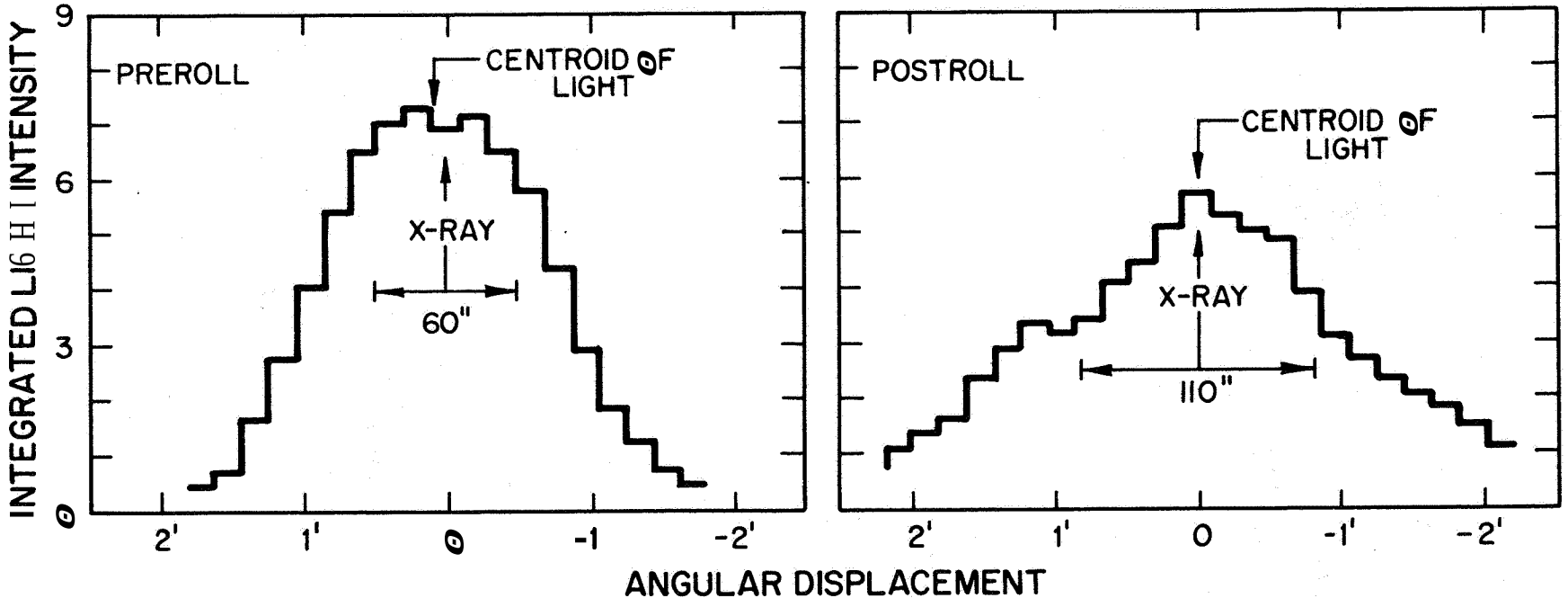

Figure 6: Visible light distributions as a function of angle along the preroll (postroll) scan direction as obtained from integrations, perpendicular to the scan direction, of the isophotes given by Woltjer (1957). The x-ray results are taken from Figure 2.

The Spectrum of Sco X-1

INTRODUCTION

The spectral characteristics of the x-rays emitted by the bright x-ray source Sco X-1 have been observed with gas filled proportional counters from Aerobee 150 rockets. Two observations were made from the White Sands Missile Range, the first on 8 March 1966, and the second on 11 October 1966. Data obtained during those flights, which have already been reported, have led to the determination of precise locations for several galactic x-ray sources [1][2][3] and the angular size of Sco X-1.[4]

X-RAY DETECTORS

In the first observation (I) the x-rays were detected in eight individual counters which utilized 0.002" entrance windows of Be mounted on a supporting frame of monel metal and a gas filling consisting of 90% Xe and 10% CH_4 at one atmosphere pressure. The total effective area after collimation was about 30 cm^2 at the center of the field of view. During the second observation (11), the x-rays were seen in 4 detectors; also having 0.002" Be entrance windows but containing a one atm gas filling of 90% Argon and 10% CH_4. The total effective area after collimation was about 400 cm^2. In both cases the field of view was triangular and the spectral analysis was based on counts recorded while the source location was between the half transmission points of the collimator. The total observation time for the data discussed here was 2.5 sec during (I) and 0.35 sec during (II). For both flights, each count event that was not accompanied by a veto signal in an anticoincidence detector was stretched to 500 microseconds with its amplitude preserved and telemetered to the ground through one of several channels. The dead time for each channel (4 for I, 2 for 11) was fixed at 1 millisecond independent of the signal amplitude. The fractional amount of "live-time" compared to the total observation time turned out to be 0.72 and 0.33 during Flights I and II respectively. However, the preamplifiers were designed to gate themselves off whenever the instantaneous rate exceeded 1 kc, as occurred during Flight II. In as much as spectral distortions were not significant below 1 kc, no spectral distortions of the detector signals should have occurred in spite of the rather large dead time corrections.

For both flights, the spectral response of the system was measured with several radioactive x-ray sources. The calibration upon which the present analysis is based was made several days prior to flight by exposing the whole detector area with several x-ray sources and receiving the telemetered signals at the ground station. These calibration data were analyzed in the same manner as the events received during the flight. In addition, the gain of the counting system up to the transmitter inputs was checked with a pulse height analyzer at regular intervals up to several hours before launch and again following the flight for the surviving detectors (all but one in Flight 11) of the recovered payloads. The gain of the system showed a stability of better than 3% before and after the flight. Changes in gain could take place during the flight as a result of temperature increases in the vicinity of the electronic instrumentation. Measurements made during Flight I showed no significant temperature rise.

The detector resolution was measured at photon energies between 1.5 and 22.1 keV. For the Xe filled detectors, a whole counter irradiation by an Fe^{55} source showed a full width at half maximum (FWHM) of 27% at 5.9 keV. Approximately 10% of the events appeared at a lower energy due to the escaping Xe *La* radiation. For the Argon detectors, the response to whole counter Fe^{55} irradiation gave a FWHM of 21% in the principal peak while 5% of the events gave rise to escaping argon Ka x-rays. For both detector types, the measured resolution was approximately proportional to the square root of the photon energy.

The calculated efficiency of both types of detectors is shown in Figure 1. The efficiency at a given energy is taken as the product of the wall transmission and the gas absorption of the incident radiation.

BACKGROUND

In addition to the discrete sources, a distinct background is observed at signal levels corresponding to a very wide range of photon energies. The background levels for Flights I and II is shown in Figure 2. The photon energy Calibration was assumed in the determination of the energy scale for these spectra although not all the events are due to photons. This background level determines our sensitivity for observing sources. The origin of the background includes several contributions. A small part can be attributed to primary cosmic ray particles which fail to produce a veto signal in the anticoincidence counters. Measurements of the spectrum produced by minimum ionizing muons showed a peak at about 8 keV and 25 keV in the argon and xenon detectors respectively; whereas in both cases, the total energy deposited in the counters should be about twice this value, This discrepancy is well known, but is unexplained. Based on data obtained during the flights themselves, the total counting rate was reduced by 50% by the presence of the anticoincidence counters.

An important source of background is undoubtedly the gamma-rays generated by the nuclear interactions of the cosmic ray primaries in the payload and in the earth's atmosphere, Each primary interaction event yields several gamma-rays. A fraction of these gamma-rays produces compton recoil electrons from the walls of the proportional counter. Consequently, the anticoincidence detector is ineffective against this kind of background, Another contribution comes from x-rays whose origin is outside the payload. This conclusion is suggested by observing the change in background level which occurred in Flight II when a door covering the entrance window to the detectors was opened. The comparison is shown in Figure 3, However, it has not been determined to what extent the earth's albedo, its radiation belts, the solar system, and large remote regions of the galaxy contribute to the x-ray background.

Although the exact origin of the background remains uncertain, it was measured and may be subtracted from the Sco X-1 spectrum to yield the net spectrum of events from that source. During Flight I, eight transits of the source were made alternately with observations of the background, amounting to a sequence of "on source", "off source" observations at almost the same conditions of vehicle .altitude and attitude. Although the background measurement of Flight II was not as precise, the signal to background ratio was much better because of the larger effective area after collimation compared to total detector volume. Hence, even a large uncertainty in the background will not have much effecton the spectrum except at the highest energies.

PROPORTIONAL COUNTERS

Efficiency and Resolution Effects

Although a gas filled proportional counter is nominally a device which produces a signal that is proportional to the quantity of energy deposited, there are various effects particularly for the detection of x-rays, that require careful consideration. These are discussed individually below for incident photons of energy E'. For the energy range of this measurement, essentially all photon interaction processes are photoelectric absorption.

Window Transmission

Incident radiation is attenuated by the detector window and elements found in the interstellar medium by photoelectric absorption. In general, the window and interstellar attenuation coefficients $\mu_s(E')$ and $\mu_w(E')$ vary as $E'^{-8/3}$ but the occurrence of absorption edges leads to discontinuous values of the coefficient. The window and interstellar transmission factors are represented by $e^{-\mu_w(E')}$ and $e^{-\mu_s(E')}$ respectively.

Gas Absorption

The photons transmitted by the interstellar medium and detector window are partially absorbed in the gas. The general trend is an increasing detector transparency or decreasing $\mu_g(E')$ with larger photon energy. The quantity $e^{-\mu_w(E')}(1 - e^{-\mu_g(E')})$ is the nominal efficiency of the detector at energy E' and is shown in Figure 1. The xenon efficiency greatly exceeds that of the argon above 8 keV. However, its resolution is poorer and its fluorescence yield larger.

The presence of absorption edges in the gas at $E' = E_K$ and $E' = E_L$ creates some complication in the analysis of proportional counter spectra. For xenon there is an L edge at 5.12 keV and a K edge at 34.7 keV, while for Argon, there is a K edge at 3.2 keV. When the energy E' of the primary x-rays exceeds that of the K(L) edge, a fluorescence x-ray containing a characteristic energy $E_{K\alpha}$ ($E_{L\alpha}$) may escape from the counter and detract from the energy deposited. A signal corresponding to an energy deposit of $E'-E_{K\alpha}$ is observed rather than the full energy E'. The overall escape probability is a function of the detector geometry and the penetration of the primary radiation into the detector. This effect is particularly severe when E' is only slightly greater than E_K. In that case $\mu(E')$ is large so that most of the primaries interact close to the front wall of the detector. The absorption by the gas of its own fluorescence radiation is about 10 times weaker and the escape probability becomes large. For example, irradiation of the xenon detectors by monochromatic 5.9 keV x-rays resulted in 10% of the events being seen at signal levels corresponding to (5.9 - 4.1) keV, where 4.1 keV is the energy of the escaping La photon.

Resolution

Due to the statistical fluctuations in the number of ion pairs produced and in the multiplication process there is a spread $e^{-(E-E')^2/\sigma^2}$ of amplitudes for a unique energy deposition. The resolution σ, in principal, is linearly proportional to the square root of the number of ion pairs and hence to the square root of the energy. Measurements of σ with several x-ray sources yielded

$$\sigma^2(E') = 0.142\ E' \qquad \text{Argon Detector}$$
$$\sigma^2(E') = 0.22\ E' \qquad \text{Xenon Detector}$$

In addition to the intrinsic minimum detector resolution there is an averaging effect because of the requirement that the data be collected in bins having a finite energy width. For purposes of making quantitative comparisons to theoretical distributions, the collection interval should be large enough to contain at least 5 events.

Unfolding of the Observed Distribution

Assuming a certain theoretical photon spectrum, $j(E')$, the effects discussed above may be incorporated into a calculation of a distribution that may be quantitatively compared to the experimental results. The calculation is indicated below for the case in which only the K edge of the gas is considered.

$j(E')$:	assumed number spectrum
$\mu_s(E')$:	interstellar attenuation
$\mu_w(E')$:	detector wall attenuation
$\mu_g(E')$:	gas absorption
$\mu'_g(E')$:	differential gas absorption per cm
$\sigma(E')$:	resolution of detector
α_k:	K shell fluorescence yield of gas
$P(E')$:	fluorescence x-ray escape probability
E_k & $E_{k\alpha}$:	K edge and energy of the K_α radiation
$E(I)$:	energy collection interval I
$DEL(I)$:	width of collection interval I
V:	counter volume
$p(\vec{r}, \vec{r}_o)$:	distance of fluorescence photon emitted from point $\vec{r}$ in the direction $\vec{r}_o$ to detector wall.

$$J(I) \int_{E(I)-DEL(I)/2}^{E(I)+DEL(I)/2} J_p(E)\,dE$$

where

$$J_p = \int_0^\infty (1-P(E'))\left(1-\alpha_k U(E'-E_k)\right) F(E')\, e^{-(E'-E)^2/\sigma^2(E')}\, dE'$$

$$+ \int_0^\infty P(E')\,\alpha_k U(E'-E_k)\, F(E')\, e^{-(E'-E_{k\alpha}-E)^2/\sigma^2(E')}\, dE'$$

$$F(E') = j(E')\, e^{-\mu w(E')} \left(1 - e^{-\mu g(E')}\right)$$

$$U(E' - E_K) = \begin{cases} 1 & E' - E_K > 0 \\ 0 & E' - E_K \leq 0 \end{cases}$$

$$P(E') = \frac{\int_\Omega \int_V e^{-\mu g'(E') X}\, e^{-\mu g'(E_{K\alpha})}\, \rho(\vec{r}, \vec{r}_0)\, dv\, d\Omega}{4\pi \int_V e^{-\mu' g(E') X}\, dv}$$

The quantities J(I) may be compared to the observed number of counts in each energy bin as a means of determining the goodness of fit achieved by an assumed spectral function j(E').

As a check upon the entire procedure a very narrow gaussian about 5.9 keV was taken as the j(E'). In Figures (4) and (5), results are compared to the pre-flight Fe^{55} irradiation as read from the telemetry records. There is generally good agreement between the theoretical and observed distributions except in the vicinity of the argon escape peak whose observed value appears anomalously large here. For all the other measurements, the ratio of counts in the escape peak to the main peak agreed much more closely with the theoretical value,

RESULTS

Three kinds of spectra were considered;

(a) $j(E') = e^{-\mu s(E')} e^{-\lambda E'/E'}$

(b) $= e^{-\mu s(E')} e^{-\lambda E'/E'^{3/2}}$

(c) $= e^{-\mu s(E')} E^{\lambda}$

and compared to the argon and xenon counter results. The first term of each expression represents a low energy cutoff due to such effects as interstellar attenuation or self absorption, Spectrum (a) is characteristic of continuum bremsstrahlung from an optically thin hot gas. Spectrum (b) was predicted by Manley in his protostar model for the x-ray sources. In that case the x-rays are produced as a result of synchrotron radiation from monoenergetic electrons. He suggests that this is the primary mechanism by which a condensing cloud of hydrogen dissipates the primordial magnetic field within it. The power law, spectrum (c), would result from the synchrotron radiation of electrons whose number energy distribution is itself a power law. For each value of the trial parameters the normalization of the theoretical to the observed distribution was determined by requiring the chi-square to be a minimum.

The two parameters λ and μ_s, were varied independently in an effort to determine the minimum chi-square. These two are not completely independent because if the large value of X (small T) is chosen, the best fit is achieved by a large value of μ_s and vice versa.

For the argon counter case, the bremsstrahlung and Manley synchrotron spectral distributions achieved a significantly better fit to the data than the power law. The chi-square test applied to the best fit with low energy attenuation gave a probability of 5% for the assumed bremsstrahlung spectrum and 3% for the Manley spectrum that the deviations between the theoretical and observed points were within the counting statistics.

Best fits to the xenon counter results did not result in a good chi-square for any of the assumed distributions. The deviations were largest at the lower photon energies. This behavior may result from a distortion of the energy calibration in that region.

The temperature and low energy attenuation parameters associated with the best fits are summarized in the table below. Comparisons between the theoretical and assumed distributions are shown in Figures (6) and (7).

Assumed Spectrum	Argon Detector		Xenon Detector	
	Temperature	Low Energy Attenuation	Temperature	Low Energy Attenuation
Bremsstrahlung	$(53.14 \pm 7.3) \times 10^6\,^{\circ}K$	1.5 ± 0.1 keV	$121 \times 10^6\,^{\circ}K$	< 1 keV
Manley	$(102 \pm 31) \times 10^6$	1.7 ± 0.1	392×10^6	< 1 keV

The low energy attenuation parameter is the energy at which the attenuation is one mean free path. The errors quoted for the argon detector are derived from an analysis of the chi-square and represent the statistical errors only, Large values of the chi-square did not justify such an analysis for the xenon data. There is a real discrepancy between the argon and xenon results. From the comparison of the absolute source intensities (discussed in the following section) there is no reason to believe that this difference is real. The discrepancy may be indicative of the quality of the measurement.

Absolute Intensity

The observed counting rates can be used to determine the absolute intensity from Sco X-1 that arrives at the top of the atmosphere. When the corrections are made for the effective area of the detectors, the collimator transmission, the collimator shadowing, and the live time, the counting rates can be related to an energy flux if a particular spectral function is assumed. However, the intensity is not very sensitive to the particular function used as long as it is not very different from the true spectrum. Here, a spectral function corresponding to bremsstrahlung from a thin hot gas at $T = 55 \times 10^6 {}^oK$ was chosen. On this basis, the absolute energy flux for the range $2 < E < 10$ keV is

$3.04 \pm 0.30 \times 10^{-7}$ ergs/cm^2-sec Argon detector

3.20 ± 10^{-7} Xenon detector

The large error in the case of the argon detector is due to the uncertainty in the dead time corrections. This result is twice that reported by Giacconi, Gursky, and Waters[6]. It is somewhat less than the intensity obtained by Grader, Hill, Seward, and Toor [7], who report a value of 5.5×10^{-7} ergs/cm^2-sec for $1 < E < 20$ keV. If the assumed spectral function isextended between those limits, the resultant intensity would be 4.75×10^{-7} ergs/cm^2-sec.

Interstellar Absorption

The best fits to the argon data include a deficiency of low energy photons beyond the expected detector wall attenuation. However, several sources of systematic errors must be considered. These are primarily uncertainties in the wall transmission and in the energy calibration. The attenuation of .002" Be is one mean free path at 1.8 keV. The actual detector wall attenuation may be somewhat greater due to the presence of a support structure in the counter interior. As a result there is a "dead region" of electric field irregularities extending into the argon a distance of .08 cm equal to about half the thickness of the support frame. This length of argon is one mean free path for

for photons of 0.73 keV. There may be additional sources of attenuation such as impurities of heavier metals in the Be and average thicknesses exceeding the nominal .002". An error of 25% in the wall thickness would be one m.f.p. at 0.75 keV. The uncertainty in the energy calibration due to changes in gain and threshold is about 0.1 - 0.2 keV. These effects could account for a great deal of the apparent low energy cutoff accompanying the best fit. In addition, no evidence of a low energy cutoff is seen from the xenon data.

A low energy cutoff is interpretable as an effect of interstellar absorption. The interstellar absorption would result from a more or less uniform density of hydrogen plus the usual associated cosmic abundance of heavier elements along the line of sight to the x-ray source. However, it may be that low energy cutoffs are attributable to peculiar features of individual sources such as self-absorption of its own x-rays (departures from an ideal optically thin hot gas) or the intervention of an unrelated gas cloud between the source and the observer.

In conclusion, although the low energy cutoff of the best fit does appear to exceed the uncertainties it is difficult to assign a quantitative value to it. In addition to the uncertainties, the magnitude of its chi-square is quite large so that one has even greater hesitancy about drawing any qualitative estimates.

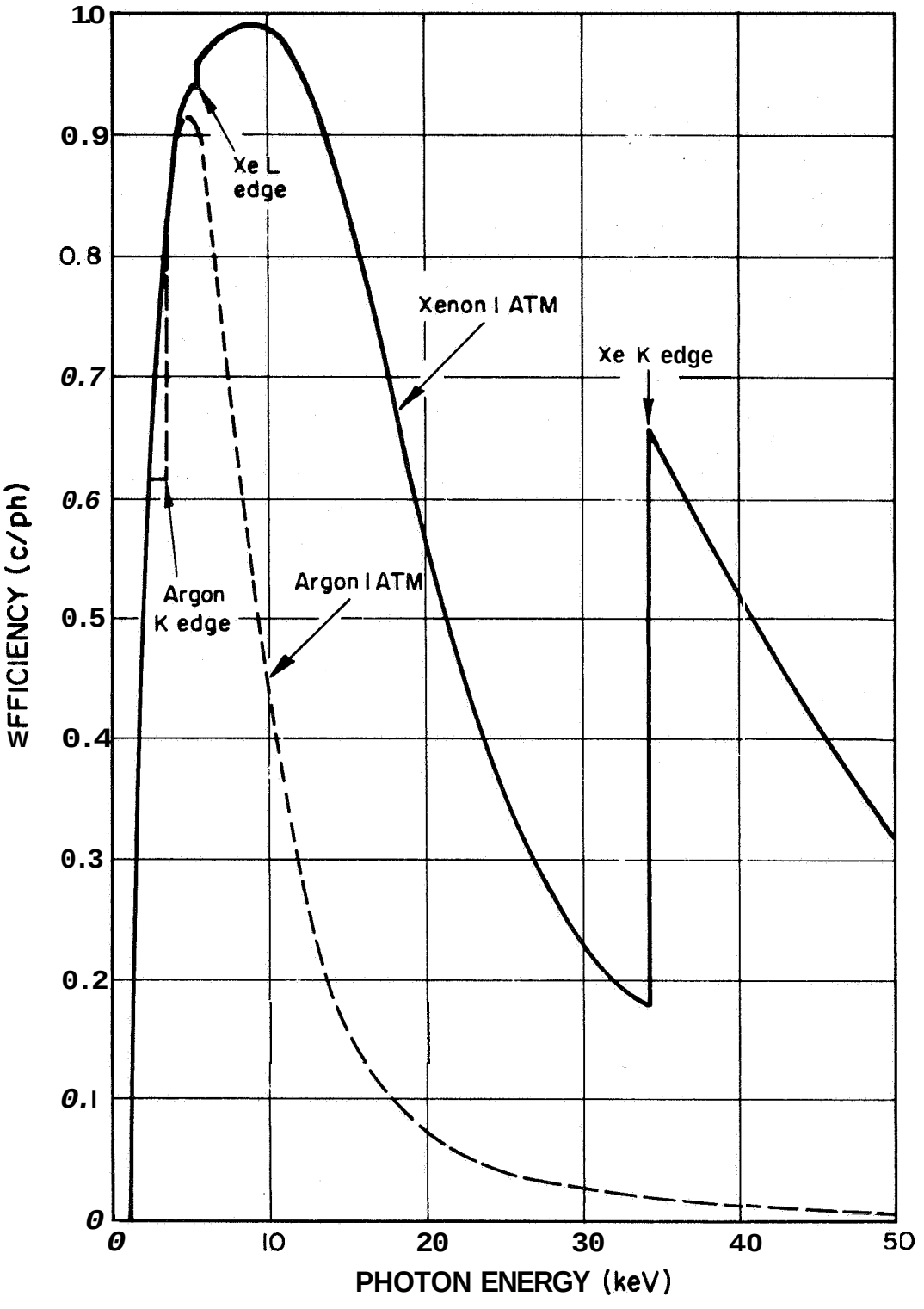

The efficiency per photon is taken as the product of $e^{-\mu w}$ the window transmission and the gas absorption, $1-\exp(-\mu'_g x_g)$.

Figure 1

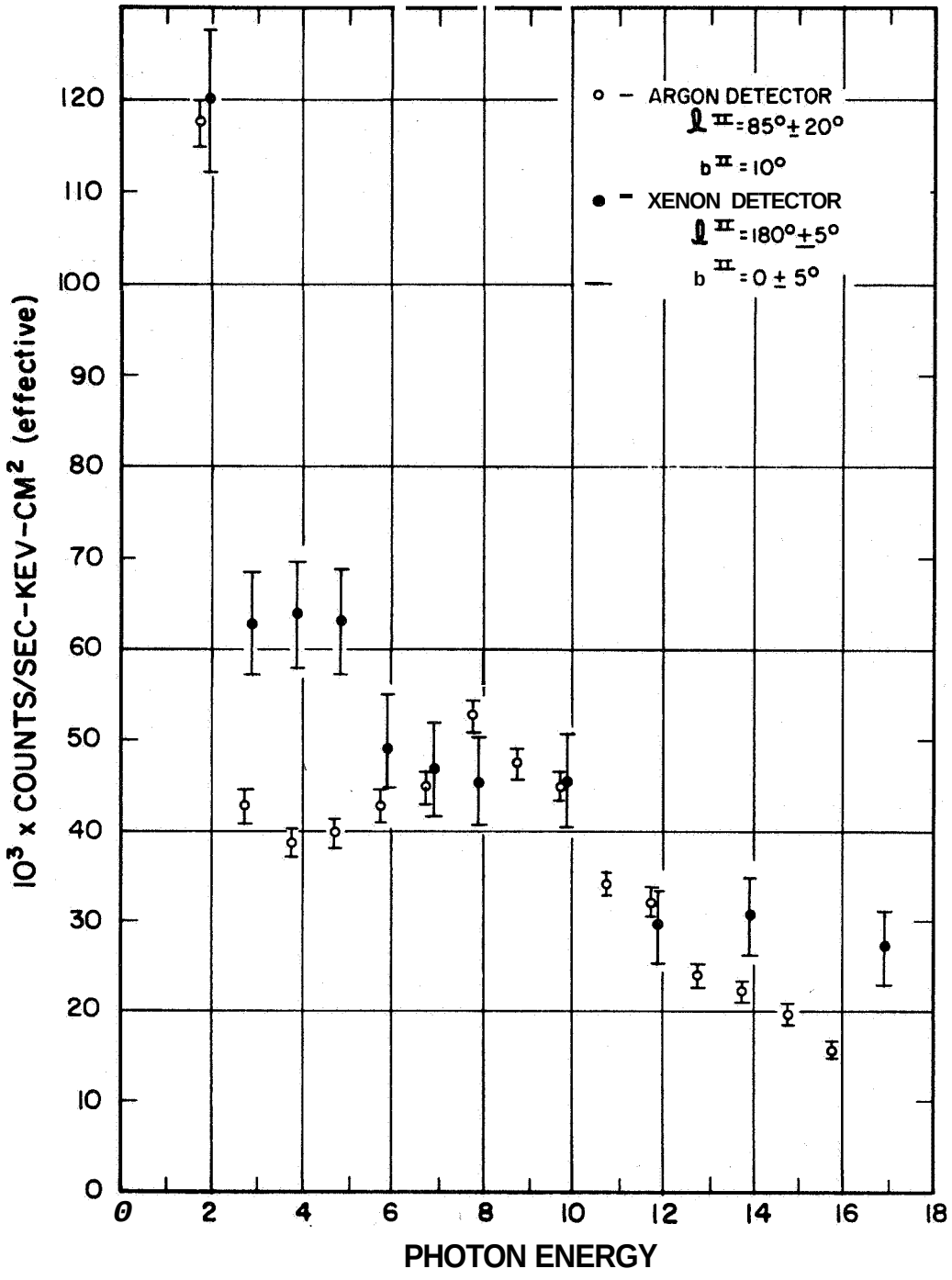

The background counting rates are determined with respect to the effective area for soft **x-rays** before collimation. The ratio of **total** front surface area including window supports was 1.85:1 and 2:1 respectively for the argon and xenon counters. Dead time corrections have not been applied.

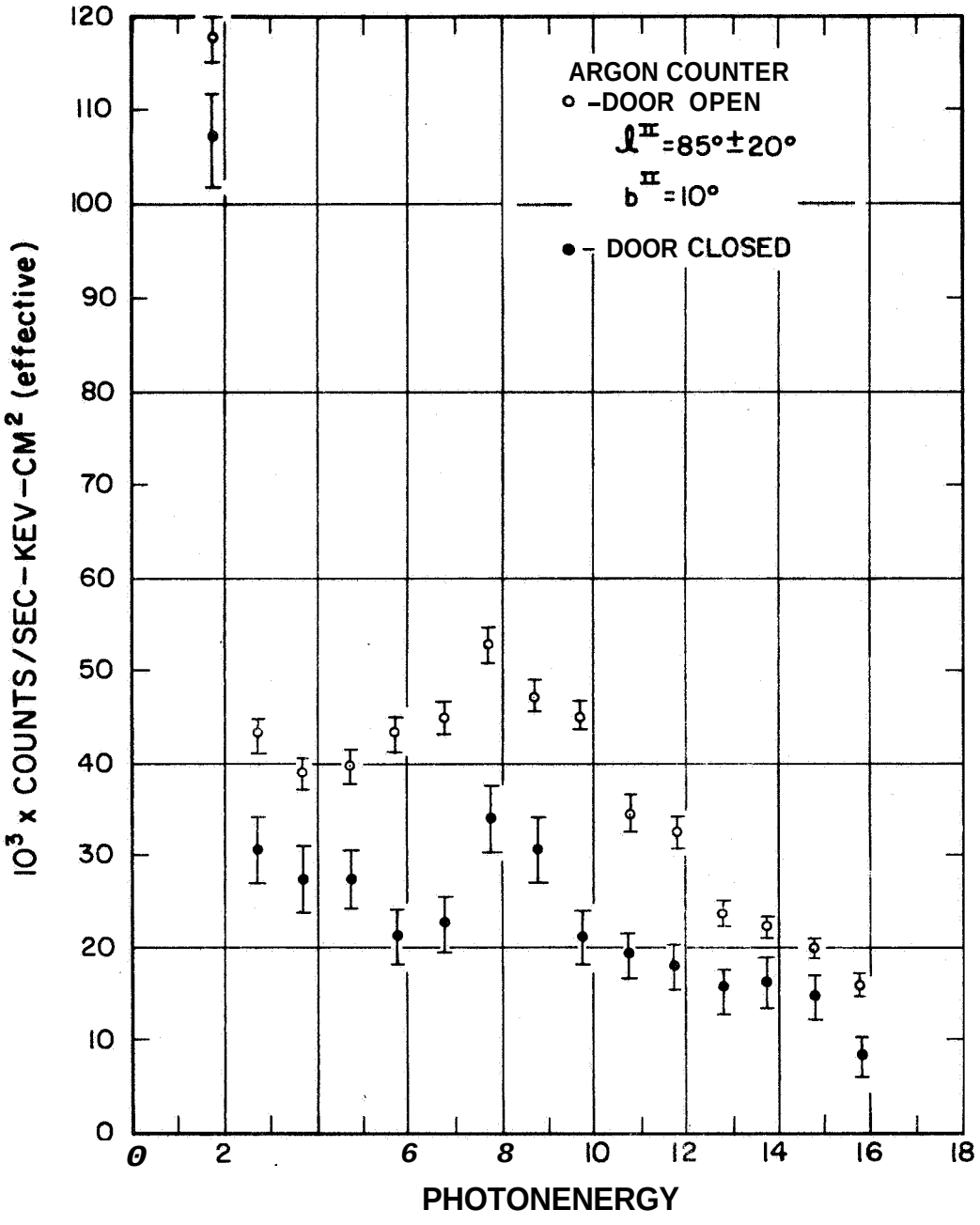

The spectral intensities during two different phases of Flight II are compared. In the "door closed" measurement, a 0.040" aluminum door covered the detectors. The "door open" measurement was made about 150 seconds later at a time when no discrete sources were believed to have been within the field of view.

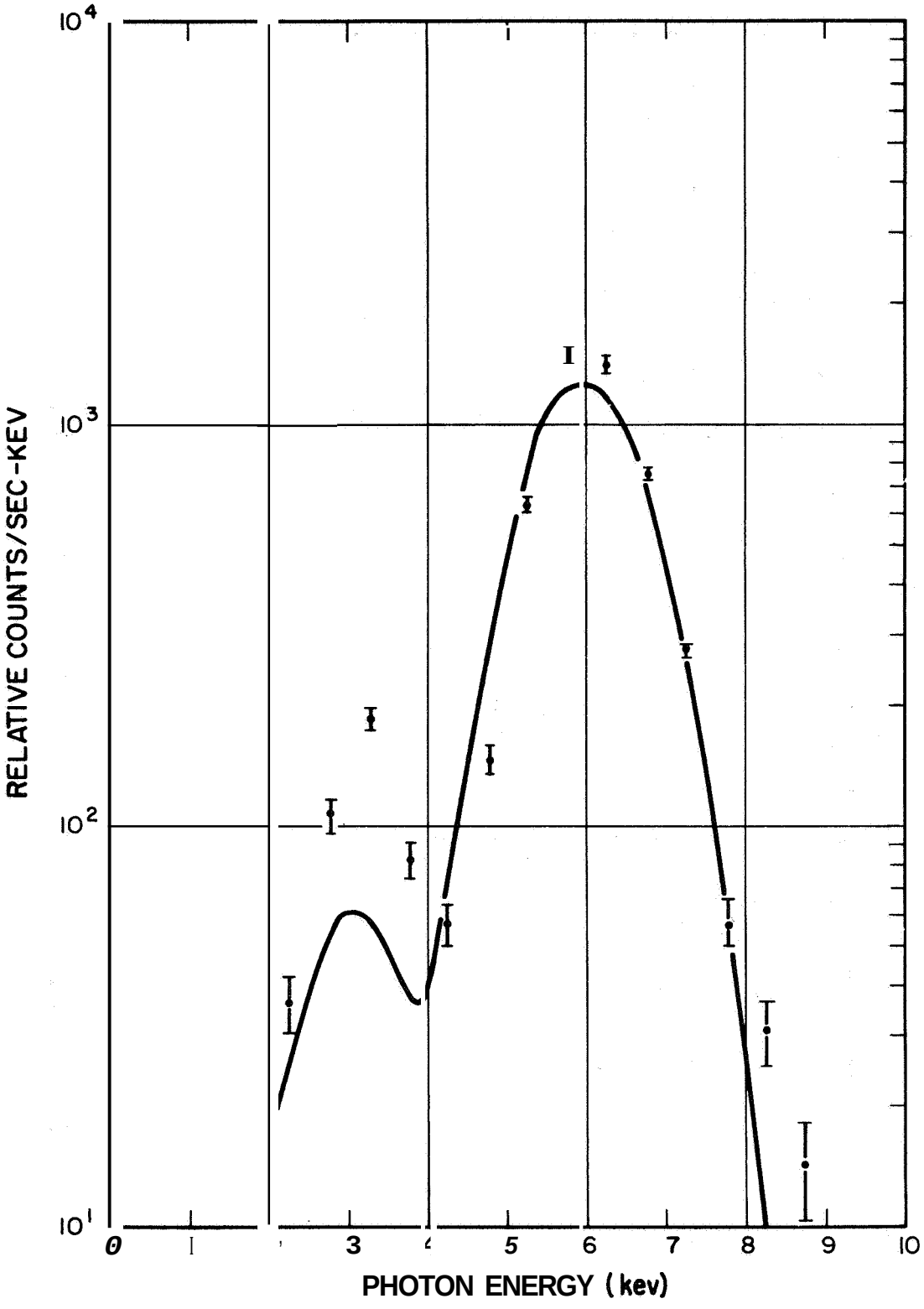

The theoretical response is based upon a photon spectrum consisting of a delta function centered about 5.9 keV incident upon a long argon (xenon) counter having a cross section of 5 cm by 5 cm. Details of the calculation are given in the text.

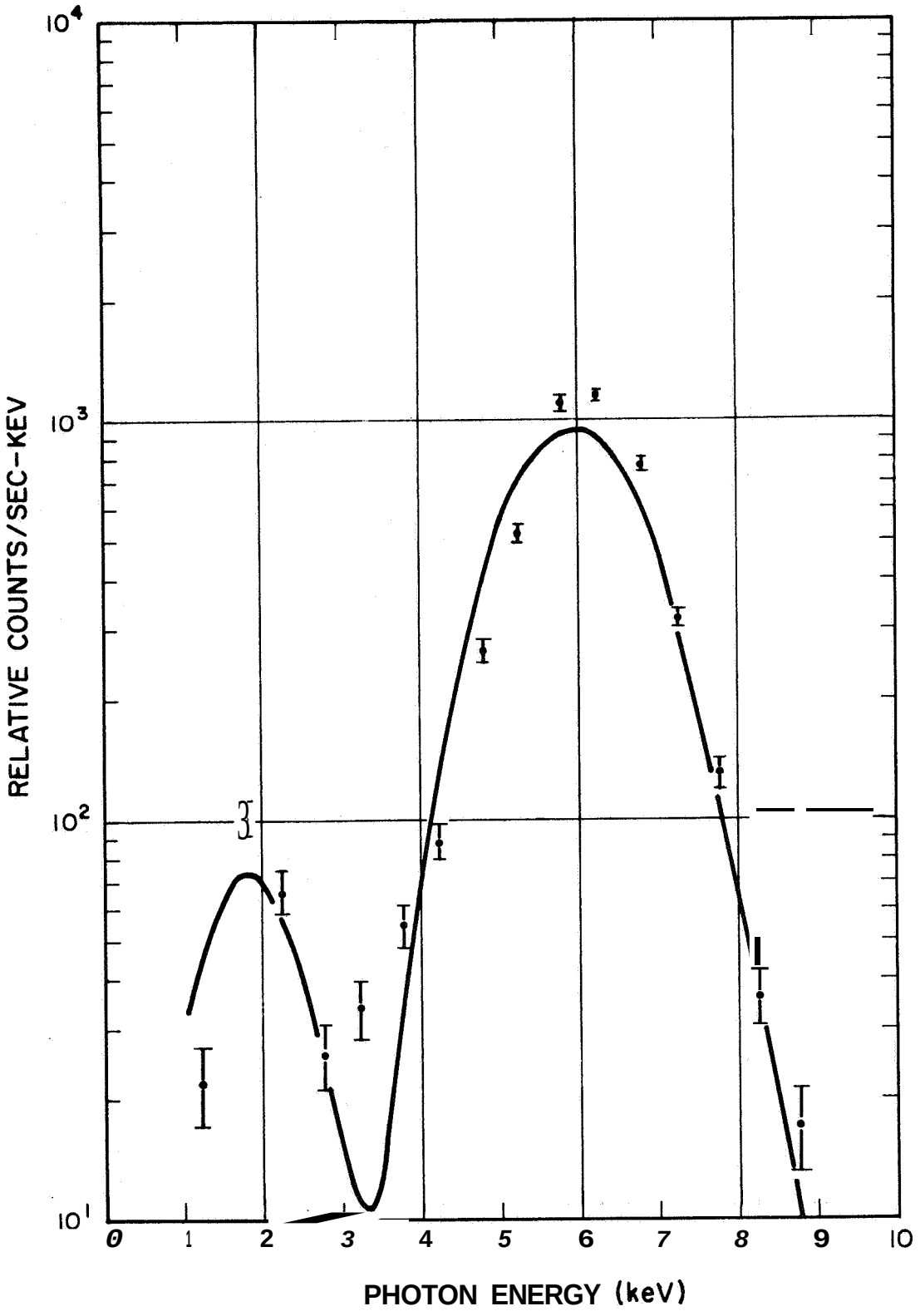

The theoretical response is based upon the photon spectrum consisting of a delta function centered about 5.9 keV'-incident upon a long argon (xenon) counter having a cross section of 5 cm x 5 cm. Details of the calculation are given in the text.

Figure 5

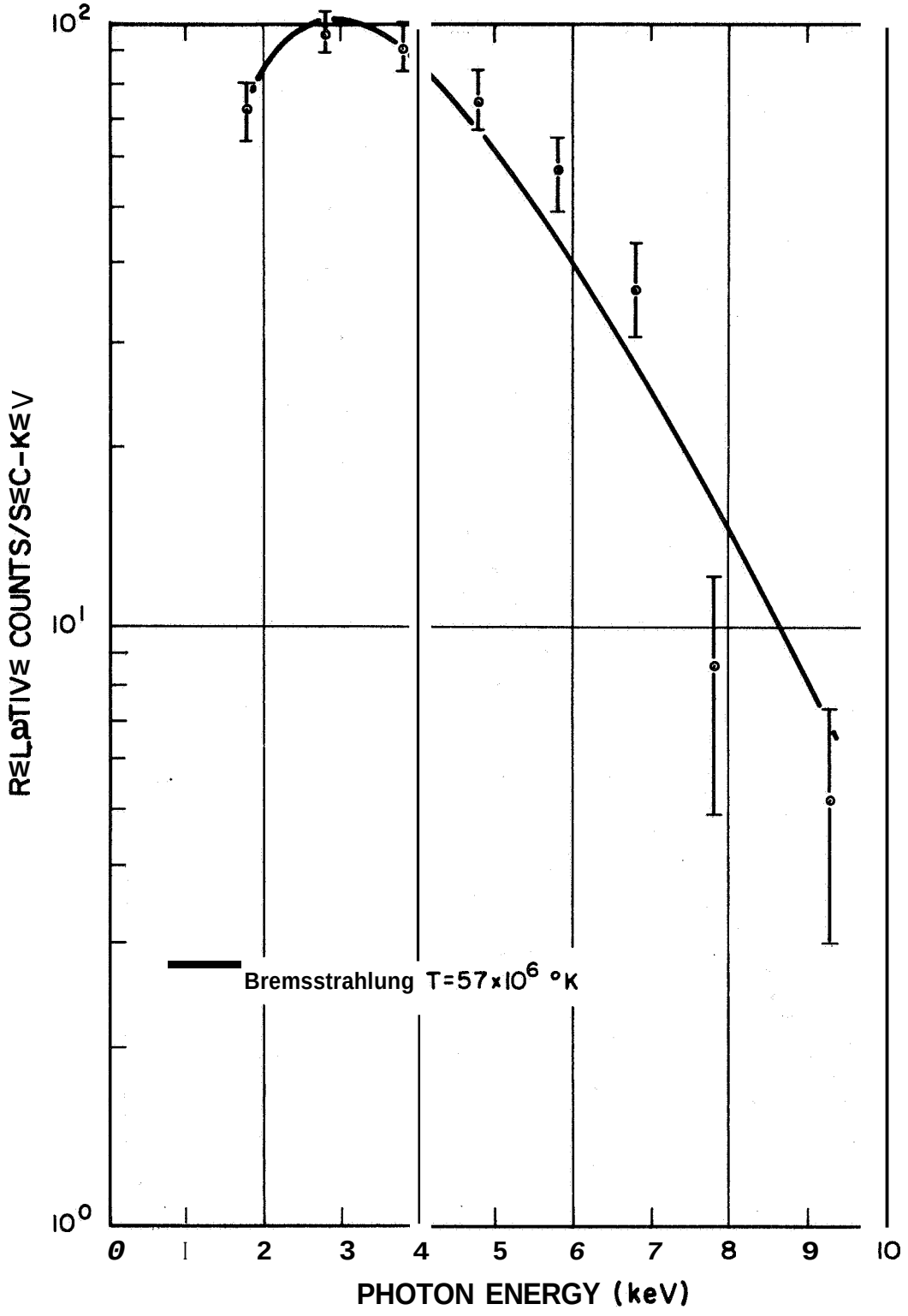

The observed and best fitting calculated spectrums are shown for the argon (xenon) counter data. The details of the calculation are described in the text. The normalization between the theoretical and observed distributions was chosen to make the chi-square minimum. The fit to the argon spectrum includes a low energy exponential cutoff that is interpretable as an effect of interstellar absorption.

Figure 6

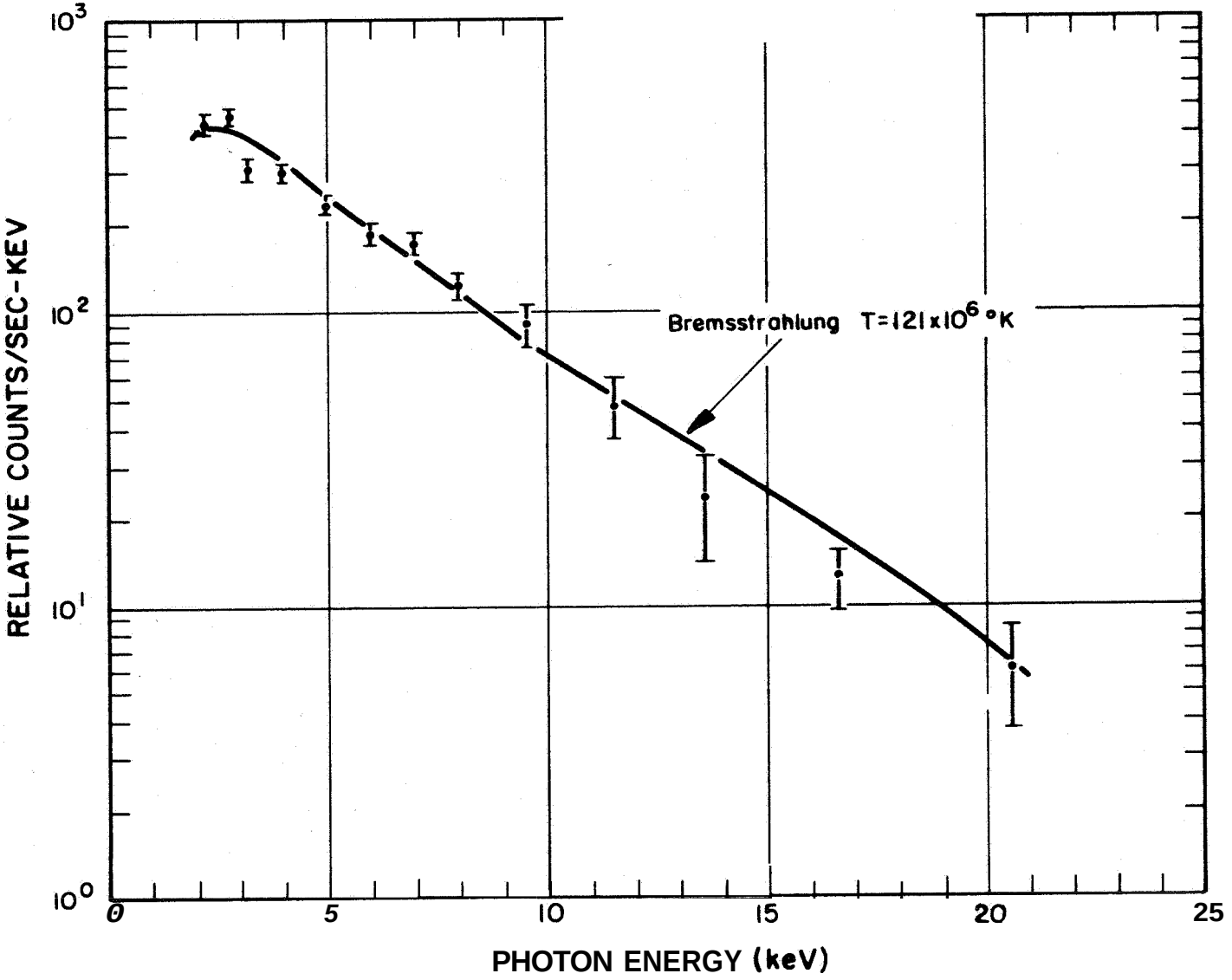

The observed and best fitting calculated spectrums are shown for the argon (xenon) counter data. The details of the calculation are described in the text. The normalization between the theoretical and observed distribution was chosen to make the chi-square minimum. The fit to the argon spectrum includes a low energy exponential cutoff that is interpretable as an effect of interstellar absorption.

Figure 7

REFERENCES

1. H. Gursky, R. Giacconi, P. Gorenstein, J.R. Waters, M. Oda, H. Bradt, G. Garmire, and B.V. Sreekantan, Astrophysical Journal 146, 311, (1966).

2. M. Oda, H. Bradt, G. Garmire, G. Spada, B.V. Sreekantan, H. Gursky, R. Giacconi, P. Gorenstein and J.R. Waters Ap. J. 148, L5, (1967).

3. R. Giacconi, P. Gorenstein, H. Gursky, and J.R. Waters (To be published in Ap. J., June 1967)

4. H. Gursky, R. Giacconi, P. Gorenstein, J.R. Waters, M. Oda, H. Bradt, G. Garmire, and B.V. Sreekantan, Ap. J. 144, 1249, (1966).

5. O. Manley, Ap. J. 144, 1250, (1966).

6. R. Giacconi, H. Gursky, and J.R. Waters, Nature 207, 572, (1965).

7. R.J. Grader, R.W. Hill, F. D. Seward, A, Toor, Science 152, 1499, (1966).

June, 1967
American Science and Engineering
11 Carleton Street
Cambridge, Massachusetts